Analyzing power and cross section distributions of the knockout reaction ^{208}Pb($\vec{p}$,2p)^{207}Tl at an incident energy of 202 MeV

R. Neveling,[1] A. A. Cowley,[1] G. F. Steyn,[2] S. V. Förtsch,[2] G. C. Hillhouse,[1] J. Mano,[3] and S. M. Wyngaardt[1]
[1]*Department of Physics, University of Stellenbosch, Private Bag X1, Matieland 7602, South Africa*
[2]*iThemba Laboratory for Accelerator Based Sciences, P.O. Box 72, Faure 7131, South Africa*
[3]*Department of Electrical Engineering and Computer Science, Osaka Prefectural College of Technology, Osaka 572-8572, Japan*
(Received 20 February 2002; published 3 September 2002)

Exclusive measurements of the cross section and analyzing power for the ^{208}Pb($\vec{p}$,2p)^{207}Tl proton knockout reaction at 202 MeV are presented for three quasifree angle pairs. Energy-sharing cross section distributions are found to be in excellent agreement with distorted wave impulse approximation (DWIA) calculations, yielding spectroscopic factors that are in reasonable agreement with (e,$e'p$) studies and theoretical expectations. The measured analyzing powers are, however, in significant disagreement with results of standard DWIA calculations that utilize the free nucleon-nucleon interaction. Analyzing power calculations are furthermore found to be insensitive to variations in the distorting potentials, different descriptions of the bound state, different energy prescriptions of the two-body interaction, and nonlocality effects. Agreement between theory and experiment is shown to improve only when the density dependence of the nucleon-nucleon interaction is incorporated within the DWIA.

DOI: 10.1103/PhysRevC.66.034602 PACS number(s): 24.50.+g, 24.70.+s, 25.40.Hs, 27.80.+w

I. INTRODUCTION

The description of quasifree proton scattering by means of the distorted wave impulse approximation (DWIA) theoretical framework [1] has proven successful in predicting angle- and energy-sharing correlation cross sections over a wide energy range (76–600 MeV) for light and medium mass targets up to ^{40}Ca [2–9]. Recently, in a study of the ^{208}Pb(p,2p)^{207}Tl reaction at an incident energy of 200 MeV [10], it was shown that the DWIA can also accurately predict cross sections for proton knockout from a heavy target, yielding spectroscopic factors that are in good agreement with results from (e,$e'p$) studies. This success, despite the severe distortion effects due to the heavy target nuclei, demonstrates the validity of the theoretical treatment of the proton distortions within the DWIA framework, at least as far as the ability to predict cross sections is concerned.

Predictions of the analyzing power of quasifree proton knockout reactions for light to medium mass targets are, however, known to be problematic. Although some success has been achieved for the spin observables for quasifree (p,2p) scattering at 200 MeV on ^{16}O and ^{40}Ca for both relativistic and nonrelativistic DWIA calculations [11–13], it is also known that experimental energy-sharing analyzing power for the very light targets ^{3,4}He at 200 MeV is substantially reduced compared to calculations [14,15]. Likewise, Carman *et al.* [16] illustrated a similar discrepancy in the angle-integrated exclusive data for ^{12}C(p,2p) at 200 MeV. For proton knockout from a ^{16}O target at 500 MeV, Miller *et al.* [17] observed that the analyzing power data are significantly reduced in comparison with non-relativistic or relativistic DWIA calculations, particularly for knockout of the $1s_{1/2}$ protons. Measurements of proton knockout at 392 MeV from the $s_{1/2}$ states in ^{6}Li, ^{12}C, and ^{40}Ca made by Hatanaka *et al.* [18] revealed a similar reduction that is a monotonically increasing function of the averaged density at which the reaction experiences its major contribution. This strongly suggests the existence of a medium effect on the nucleon-nucleon interaction, as would be intuitively expected.

On the other hand, Miller *et al.* [17] showed that, although the inclusion of density-dependent interactions in the DWIA calculations improved agreement with the data, it still does not resolve the discrepancy satisfactorily. This result supports the conclusion of Noro *et al.* [19], who showed that the distinct density dependence of the reduction in analyzing power in ^{6}Li, ^{12}C, and ^{40}Ca is only qualitatively reproduced when incorporating similar density-dependent DWIA calculations as used in Ref. [17].

In order to investigate the origin of the overprediction of the analyzing power, it is useful to compare the observed phenomenon with the situation for different target nuclei, especially for *s*-state knockout. For *s*-state knockout the relation between the spin observables of the (p,2p) reaction and that of free nucleon-nucleon scattering is expected to be a relatively simple one, whereas the effective polarization of the bound nucleons (the so-called Maris effect [20]) makes the relation somewhat complicated in the case of $l \neq 0$ states [18]. The prominence of *s*-state knockout in the case of a ^{208}Pb target would then make it an ideal candidate for further study. Since previous cross section results [10] suggested that the available theoretical framework could successfully be applied to knockout from heavy target nuclei, a high-resolution coincidence measurement of energy-sharing cross section and analyzing power of the ^{208}Pb($\vec{p}$,2p)^{207}Tl knockout reaction at 202 MeV was undertaken with the aim to separate the $3s_{1/2}$ ground state from the first three excited states of ^{207}Tl.

The following section (Sec. II) elaborates on the details related to the experimental arrangement and the data analysis. Details of the theoretical calculations are given in Sec. III. The results are presented in Sec IV, followed by the summary and conclusion in Sec. V.

 ©2002 The American Physical Society

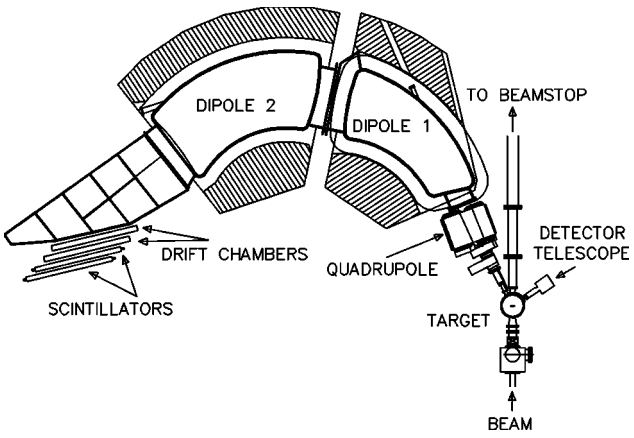

FIG. 1. An overhead view of the detector configuration. High-energy protons were detected on the beam-left side with the $K=600$ QDD magnetic spectrometer, shown here with its associated focal plane detectors. A ΔE-E detector telescope, consisting of a Ge stopping E detector and a Si ΔE detector, detected the lower-energy protons on the beam-right side.

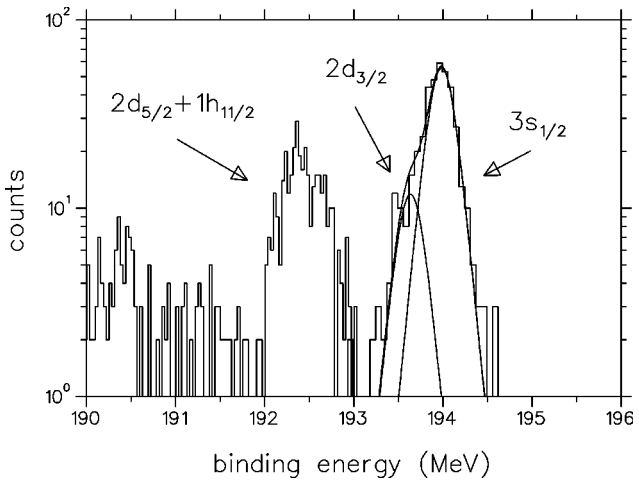

FIG. 2. A typical binding-energy spectrum for the ^{208}Pb$(\vec{p},2p)^{207}$Tl knockout reaction at 202 MeV. The states relevant to this study are indicated.

II. EXPERIMENTAL PROCEDURE

The experimental work was performed with the separated sector cyclotron facility of the iThemba Laboratory for Accelerator Based Sciences (formerly known as the National Accelerator Center), Faure, South Africa. A proton beam of energy 202 ± 0.5 MeV, polarized normal to the scattering plane and with beam intensities of up to 30 nA, was delivered to the magnetic spectrometer experimental area. Energy spread of the beam was limited to an estimated 125 keV by emittance-limiting slits in the beamline. Beam polarization was switched from up to down in 10-sec intervals in order to minimize systematic errors in analyzing power measurements. The typical polarization ranged between 70% and 80%, with the difference in the polarization between the two orientations routinely less than 5%, and always less than 15%.

Protons were detected in coincidence with a $K=600$ QDD magnetic spectrometer (where K is the well-known magnetic spectrometer constant) and a ΔE-E detector telescope, mounted coplanar on opposite sides of the incident beam. The detector telescope consisted of a 1000-μm silicon surface barrier detector and a 15-mm N-type high-purity planar germanium detector. Energy-sharing cross sections and analyzing powers were measured for three angle pairs close to the quasifree condition, i.e., angle pairs at which knockout of bound protons at rest in the target nucleus is kinematically accessible. Limitations due to the finite thickness of the germanium crystal, the design of the scattering chambers as well as hydrogen contamination of the ^{208}Pb targets restricted measurements to the angle pairs $(\theta_{K600},\theta_{telescope})=(22°,-62.3°)$, $(28°,-54.6°)$, and $(33°,-49.7°)$, where θ_{K600} and $\theta_{telescope}$ denote the scattering angles at which the magnetic spectrometer and telescope are respectively positioned. The sign (positive or negative) indicate respective angles on opposite sides of the incident beam. A layout of the experimental setup is shown in Fig. 1. The accelerator and main details of the experimental equipment have previously been described elsewhere [21].

Particle identification in the telescope was achieved through standard ΔE-E techniques, while particle identification in the spectrometer was achieved through time-of-flight selection and ΔE-ΔE techniques using the two scintillator detectors in the focal plane of the spectrometer. Calibration of the germanium detector for the early experimental runs was achieved by making a coincident measurement of the $H(p,p)$ reaction at 202 MeV for the elastic scattering angle pair $(32.7°,-54.6°)$. Later calibrations were based on various elastic and inelastic scattering reactions from H, ^{12}C, and ^{197}Au, obtained at different angles for a 66.5-MeV proton beam. All the calibration parameters were then optimized in the off-line analysis by ensuring a sharp as possible peak in the binding-energy spectrum for proton knockout. The silicon detector was calibrated with a ^{228}Th α source, and the magnetic spectrometer by means of $p+^{12}$C elastic and inelastic scattering with a 202-MeV proton beam.

Two self-supporting isotopically enriched ^{208}Pb target foils of different thicknesses were used. The thicker of the two was 7.7 ± 0.54 mg cm^{-2} thick, and consisted of 98% isotopically enriched ^{208}Pb. The thinner ^{208}Pb target, enriched to 99%, had a thickness of 0.74 ± 0.04 mg cm^{-2}. The thinner target was chosen for runs aimed at a better energy resolution, whereas the thicker target was chosen to obtain a higher count rate in other runs.

A typical binding-energy spectrum is shown in Fig. 2. Due to straggling and other effects the energy resolution achieved for neither target was sufficient to achieve complete online separation of the $3s_{1/2}$ ground state of ^{207}Tl from the $2d_{3/2}$ first excited state, or to resolve the $2d_{5/2}$ and $1h_{11/2}$ states. However, the data were still of sufficient quality, having a full width at half maximum of 310 keV for the thin target and 480 keV for the thick target, to allow the extraction of data for knockout to respectively the $3s_{1/2}$ and the $2d_{3/2}$ states. This was achieved by means of a peak-fitting procedure constrained by the known separation energies of the proton bound states, as found in Ref. [22]. Sufficient data for peak deconvolution was acquired only for the data sets of

the angle pairs $(28°,-54.6°)$ and $(22°,-62.3°)$. Lower statistics for the $2d_{5/2}$ and $1h_{11/2}$ states, together with the fact that the contribution of the $1h_{11/2}$ state to the sum of the two states is negligible over most of the observed energy range anyway, did not make efforts to obtain results for each of these states separately worthwhile. For the angle pair $(22°, -62.3°)$ the accuracy of cross section distributions for the resolved states was lost due to electronic malfunction, but this did not affect the measurement of the analyzing power.

The analyzing power (A_y) was obtained by taking the different polarizations of the upward and downward polarized beams into account through the relationship

$$A_y = \frac{C^{\uparrow} - C^{\downarrow}}{C^{\uparrow} p^{\downarrow} + C^{\downarrow} p^{\uparrow}}. \quad (1)$$

The quantity $C^{\uparrow(\downarrow)}$ denotes the corrected quasifree-scattering yield for upwards (downwards) polarized incident protons, and $p^{\uparrow(\downarrow)}$ represents the degree of upward (downward) polarization. The systematic error for the cross section results, mainly due to uncertainty in target thickness, is estimated to be 8%. Systematic errors in the analyzing power, due to an uncertainty in the measured polarization, were found to be negligible compared to the analyzing power statistical errors.

III. THEORETICAL CALCULATIONS

The ability to accurately predict cross sections and analyzing powers within the DWIA theoretical framework depends on a good description of the distortion mechanism affecting the incoming and two outgoing nucleons, an accurate description of the bound nucleon and also a sound understanding of the nucleon-nucleon interaction inside the nuclear field. It is therefore instructive to investigate the sensitivity of the theoretical calculations to these three essential components of the DWIA.

Theoretical calculations were performed with the nonrelativistic DWIA formalism [23,24], i.e., treating the nucleon-nucleon interaction nonrelativistically while the kinematics of the knockout process is treated relativistically, using a recent version of the computer code THREEDEE [25]. The DWIA formalism gives the transition amplitude as a product of a distorted wave momentum distribution and a two-body nucleon-nucleon amplitude, which is half off the energy shell [26]. However, in the case of the present study, with a projectile energy of 202 MeV, a Q value of 8.013 MeV, and experimental conditions emphasizing minimum recoil momentum, approximating the half off-shell two-body amplitude by an on-shell two-body amplitude is regarded as reasonable. This nevertheless leads to ambiguities in the evaluation of the nucleon-nucleon interaction regarding the assignment of the energy in the two-body scattering system. Two different energy prescriptions are routinely used: in the final energy prescription the effective laboratory kinetic energy for the two-particle interaction is calculated with the final state proton kinematics. The initial energy prescription, on the other hand, employs the initial state proton kinematics to calculate the effective kinetic energy.

Distorted waves for the incident and outgoing protons were generated by solving the Schrödinger equation with complex optical potentials, and results given by three different optical potential sets were investigated. These were a set generated by a Schrödinger equivalent reduction of the global Dirac analysis of Hama *et al.* [27] (the second parametrization), a set from the work of Schwandt *et al.* [28], and the parameters of Nadasen *et al.* [29]. Nonlocality effects for the distorted waves were incorporated according to a simple parametrization of the nonlocal potentials by Perey and Buck [30] in terms of the above local potentials.

The radial part of the single-particle bound-state wave function was generated as a solution of the Schrödinger equation with a Woods-Saxon potential. The various bound state parameter sets [10,24,31–33] that were utilized are generally constrained by electron scattering data. The nonlocality of the bound-state wave functions was treated similarly to the treatment of nonlocality in the distorted waves.

The two-body interaction in the DWIA is approximated by the interpolation of available phase shifts [34] determined from nucleon-nucleon elastic scattering. Calculations for density-dependent nucleon-nucleon interactions, complementing the above density-independent calculations, were performed with the empirical effective interaction parametrized by Kelly and Wallace [35]. A second, alternative approach, involved a t matrix modified for an effective nucleon mass, following the procedure proposed by Horowitz and Iqbal [36].

Finally, for comparison relativistic DWIA calculations were also performed with the code RELP2P [37], which employs the finite-range RDWIA model of Mano and Kudo [38]. In this model the single-particle bound-state wave functions are calculated from relativistic mean fields produced by the Dirac-Hartree model. Distorted wave functions are calculated from microscopic optical potentials obtained by folding nuclear densities with the nucleon-nucleon interaction of Horowitz [39]. In all the calculations it was assumed that the ground state and first three excited states of ^{208}Pb are unfragmented, which is a reasonable assumption especially for the $3s_{1/2}$ and $2d_{3/2}$ states [32,40].

IV. RESULTS AND DISCUSSION

Experimental triple differential cross section and analyzing power results for the unseparated valence states for all three the measured angle pairs are displayed and compared to theoretical calculations in Figs. 3 and 4. The data are presented as a function of the energy of the most energetic proton in the final state, i.e., the proton detected in the magnetic spectrometer. Panels in different rows denote results for different angle pairs, and knockouts to different combinations of states for these various angle pairs are found in panels in the different columns. The error bars shown represent the statistical uncertainty, and the arrows indicate the position of minimum recoil. Theoretical results for the combined knockout to the various states are calculated by weighting contributions from the different states with relative spectroscopic factors (RSF), as obtained by Royer *et al.* [41] in a ^{208}Pb$(d,^3$He$)^{207}$Tl study. For the combined knockout from n

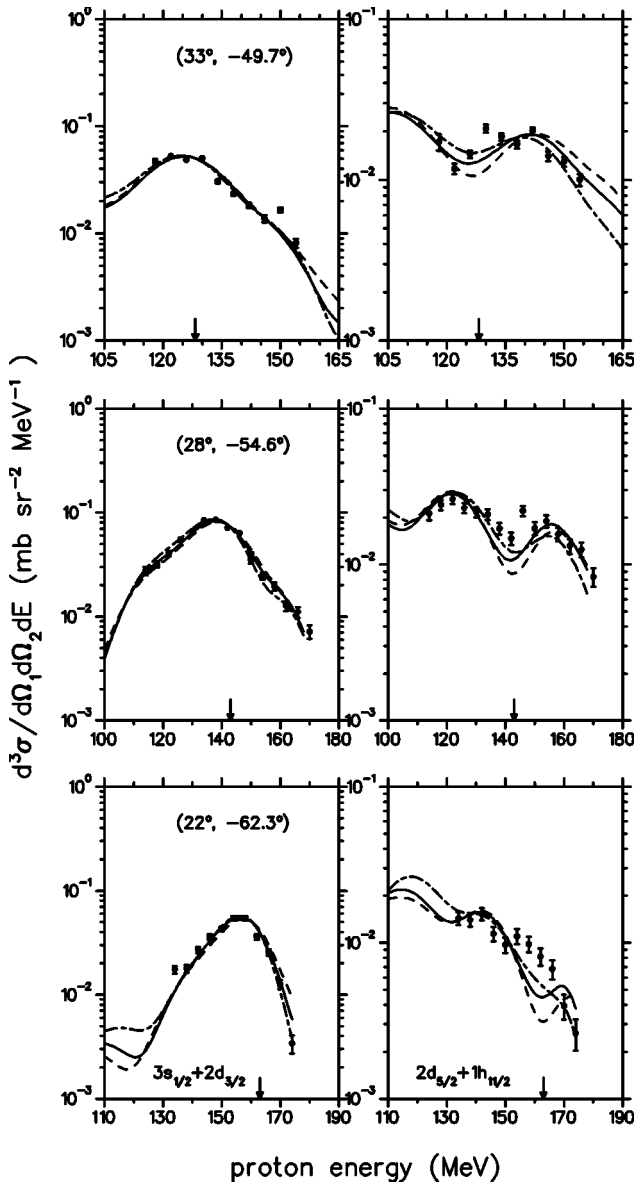

FIG. 3. Energy-sharing cross sections for the ^{208}Pb($\vec{p}$,2p)^{207}Tl reaction at 202 MeV for the unresolved valence states at the angle pairs indicated. The curves represent DWIA predictions for the free nucleon-nucleon interaction and distorting optical potential parameter sets of Schwandt *et al.* [28] (solid line), Nadasen *et al.* [29] (dashed line), and Hama *et al.* [27] (dot-dashed line). The DWIA calculations shown are plotted with the spectroscopic factors from Table I, multiplied by the shell model value of $2j+1$. The arrows indicate the position of minimum recoil.

states the effective theoretical analyzing power is thus given by

$$A_{\mathrm{eff}}=\frac{\sum_{i=1}^{n} d^3\sigma^i \cdot A_y^i \cdot RSF^i}{\sum_{j=1}^{n} d^3\sigma^j \cdot RSF^j}, \tag{2}$$

and the effective triple differential cross section by

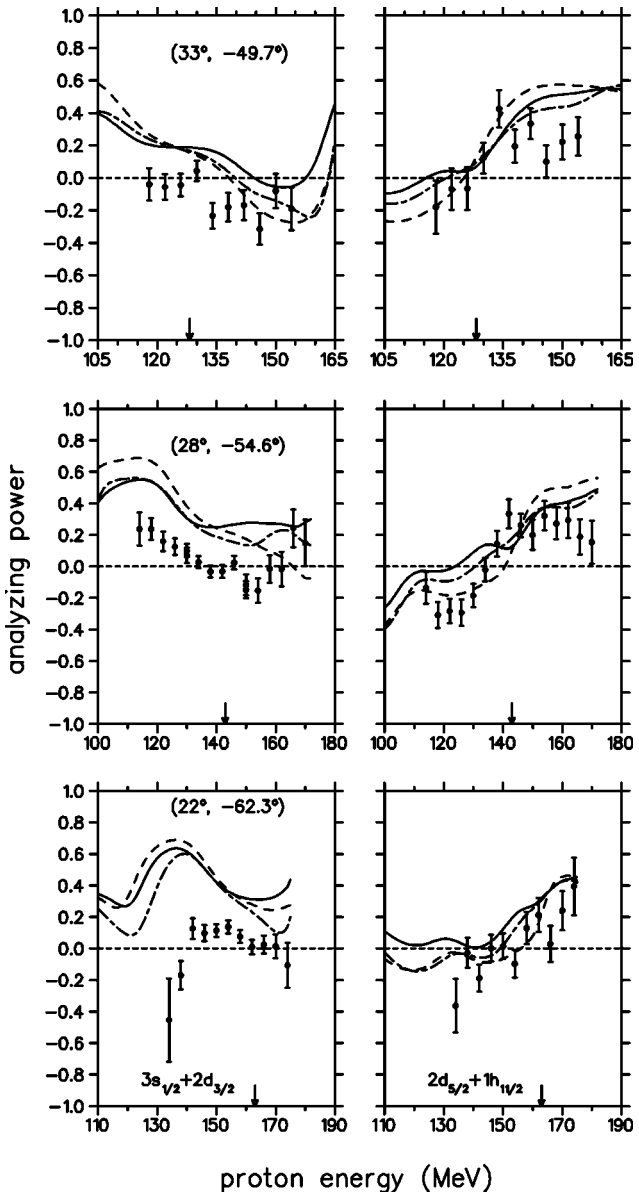

FIG. 4. Energy-sharing analyzing powers for the ^{208}Pb($\vec{p}$,2p)^{207}Tl reaction at 202 MeV for the unresolved valence states. The details of the calculations are the same as in Fig. 3.

$$d^3\sigma_{\mathrm{eff}}=\sum_{i=1}^{n} d^3\sigma^i \cdot RSF^i, \tag{3}$$

where $d^3\sigma^i$, A_y^i, and RSF^i, respectively, represents the triple differential cross section, analyzing power, and relative spectroscopic factors (normalized to either $RSF^{3s_{1/2}}$ or $RSF^{2d_{5/2}}$) for knockout to state i.

The experimental results and theoretical calculations for the separated ground and first excited state are displayed in Fig. 5, along with the results for the pair of states ($2d_{5/2}+1h_{11/2}$). For reasons mentioned previously, analyzing power data for the $3s_{1/2}$ and $2d_{3/2}$ single state knockout exists only for the two angle pairs (22°, −62.3°) and (28°, −54.6°), and the corresponding cross section data only for the latter angle pair. Note that whereas in Figs. 3 and 4 the

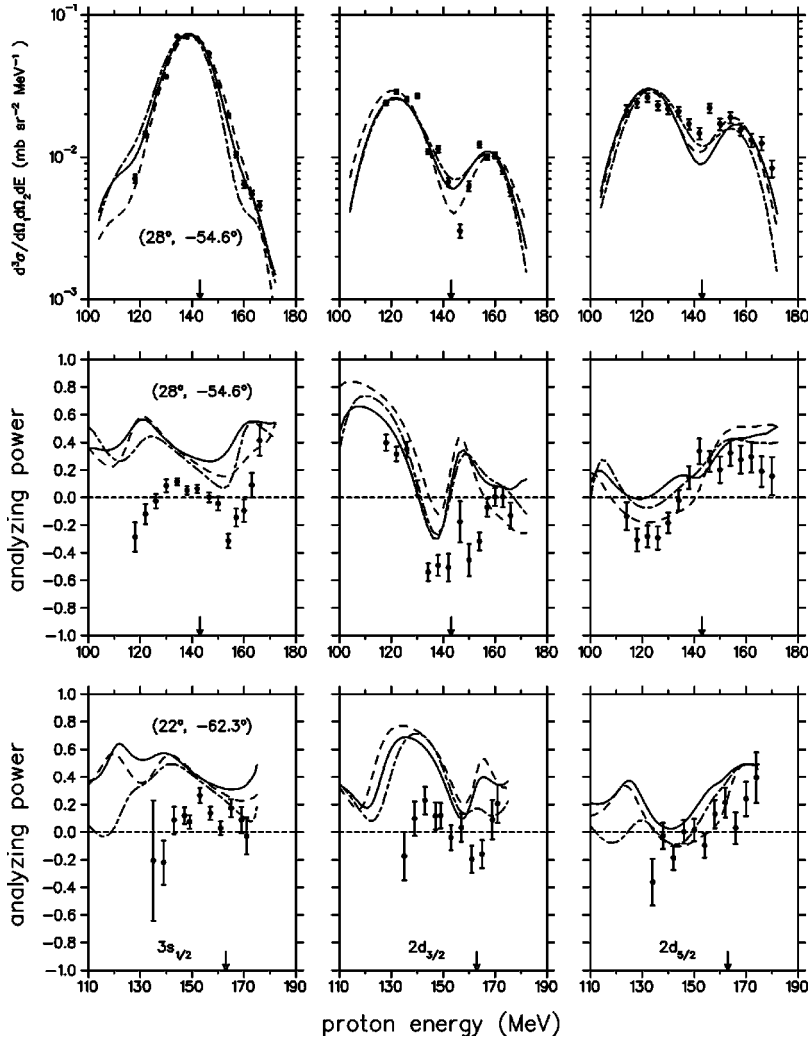

FIG. 5. Analyzing power and cross section energy-sharing distributions for the ^{208}Pb$(\vec{p},2p)^{207}$Tl reaction at 202 MeV for the resolved $3s_{1/2}$ and $2d_{3/2}$ states. Note that the results for the unresolved $(2d_{5/2}+1h_{11/2})$ states are compared to calculations for the $2d_{5/2}$ state only. Details of the calculations are the same as in Fig. 3.

experimental results of the $(2d_{5/2}+1h_{11/2})$ states were compared to theoretical values for the combination of the two states, the theoretical values presented in Fig. 5 are for the $2d_{5/2}$ state only. A comparison of DWIA calculations for only the $2d_{5/2}$ state to the result of the combination of the two states clearly illustrates that the contribution of the $1h_{11/2}$ state is negligible small over most of the energy range covered in this experiment, and can subsequently be ignored.

The theoretical calculations in Figs. 3, 4, and 5 represent standard nonrelativistic DWIA calculations performed with the bound state parameter set of Mahaux and Sartor [31], and the various distorting optical potentials noted in the previous section. The Perey Buck damping term [30] with nonlocality range of $\beta=0.85$ fm was used to incorporate nonlocality effects for the distorted and bound state waves. The free nucleon-nucleon interaction in the final energy prescription was employed to evaluate the nucleon-nucleon scattering amplitude.

From Figs. 3 and 5 it is clear that the cross sections are adequately predicted by the DWIA calculation, for all three optical potential sets used. Good overall shape agreement is found between experiment and theory for the mixed state results of all the angle pairs, as well as for the $3s_{1/2}$ and $2d_{3/2}$ results for the angle pair $(28°,-54.6°)$. Furthermore, the experimental spectroscopic factors from Table I compare favorably with those from the literature, listed in Table II. Differences between the spectroscopic factors for different optical potential sets are ascribed mostly to the differences in the

TABLE I. Experimental spectroscopic factors (normalized to a maximum value of unity) extracted from the standard DWIA calculation that employs the Hama *et al.*'s [27] distorting optical potential. The error indicates experimental systematic errors.

Angle pair	all states	$3s_{1/2}+2d_{3/2}$	$3s_{1/2}$	$2d_{3/2}$	$2d_{5/2}+1h_{11/2}$	$2d_{5/2}$
$(22°,-62.3°)$	0.65 ± 0.05	0.59 ± 0.04	−	−	0.56 ± 0.04	0.70 ± 0.04
$(28°,-54.6°)$	0.90 ± 0.07	0.85 ± 0.07	0.82 ± 0.07	0.84 ± 0.07	0.61 ± 0.05	0.67 ± 0.05
$(33°,-49.7°)$	0.52 ± 0.04	0.45 ± 0.04	−	−	0.48 ± 0.04	0.51 ± 0.04

TABLE II. Existing spectroscopic factors for the $3s_{1/2}$ state.

Reference	Spectroscopic factor
[10] $(p,2p)$	$0.7-0.8$
[42] $(e,e'p)$	0.65
[43] $(e,e'p)$	0.71
[44] $(e,e'p)$	0.70
[45] theory	0.71 ± 0.1
[46] theory	0.69

strength of the imaginary part of the central potential. For the analyzing power results, serious discrepancies are evident from Figs. 4 and 5. Theoretical calculations, especially for results involving the $3s_{1/2}$ state, overestimate the measured analyzing power considerably, irrespective of the optical potential set used. However, better agreement is achieved for the $(2d_{5/2}+1h11_{1/2})$ results.

Extensive calculations were performed to test the sensitivity of the analyzing power to the choice of energy prescription of the nucleon-nucleon interaction, the influence of nonlocality, as well as the choice of bound state parameter sets. While it is known [5,47] that nonlocality effects and different bound state parameter sets cause amplitude variations in calculated cross sections, the analyzing power for the ^{208}Pb$(\vec{p},2p)$ reaction reveals little or no sensitivity to these aspects of the calculation. Calculations for the initial and final energy prescriptions also revealed negligible differences.

A. Density dependence of the nucleon-nucleon interaction

The analyzing power for the exclusive $(p,2p)$ measurement has contributions from both the quasifree reaction (target-nucleon momentum distribution, distortion effects on the incoming and final state protons) as well as the underlying spin correlation coefficient of the nucleon-nucleon interaction. In this section, density-dependent modifications to the latter are investigated.

The radial localization of the knockout reaction provides insight into the possible magnitude of medium modifications on the quasifree reaction. This is investigated by calculating the contribution of the triple differential cross section as a function of radial distance, as described in Ref. [48]. The histograms shown in Fig. 6 represent the radial distribution of contributions to the DWIA cross section at the point of minimum recoil, arbitrarily normalized to comparable magnitudes for comparison purposes. The smooth solid curves represent the bound-state radial wave functions, shown for radial reference. Although it is clear that the reaction is localized mainly on the nuclear surface, *s*-state knockout displays a somewhat larger contribution from the nuclear interior than the *d* states. This suggests that it could be more susceptible to medium modification of the nucleon-nucleon interaction. A definite trend is also clearly observed for the *s* state, where the contribution to the reaction from the nuclear interior is decreasing with increasing scattering angle θ_{K600}, leading to a possible corresponding decrease in sensitivity to medium effects for an increase in the primary scattering angle. Note that this conclusion regarding the magnitude of the contribution from the nuclear interior applies only at or near the quasifree point. For example, at recoil momentum $p_{recoil}\geqslant 80$ MeV/c calculations predict an increase in the contribution to the reaction at smaller radii, compared to calculations at the quasifree point.

Calculations with the density dependence of the nucleon-nucleon two-body interaction included are compared with calculations with the free interaction, as well as with experimental values in Figs. 7 and 8. The distorting optical model potential for these calculations was obtained from the work

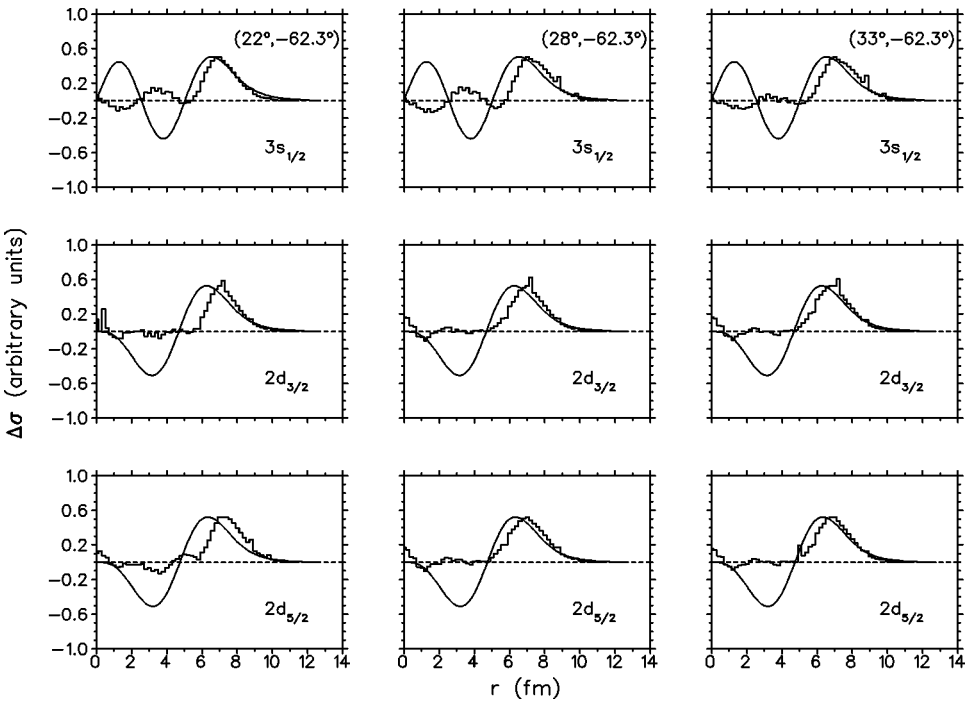

FIG. 6. Histograms depicting the radial distribution of contributions to the DWIA cross section $(\Delta\sigma)$ at the quasifree point for three valence states of ^{208}Pb. The smooth solid lines represent bound state radial wave functions.

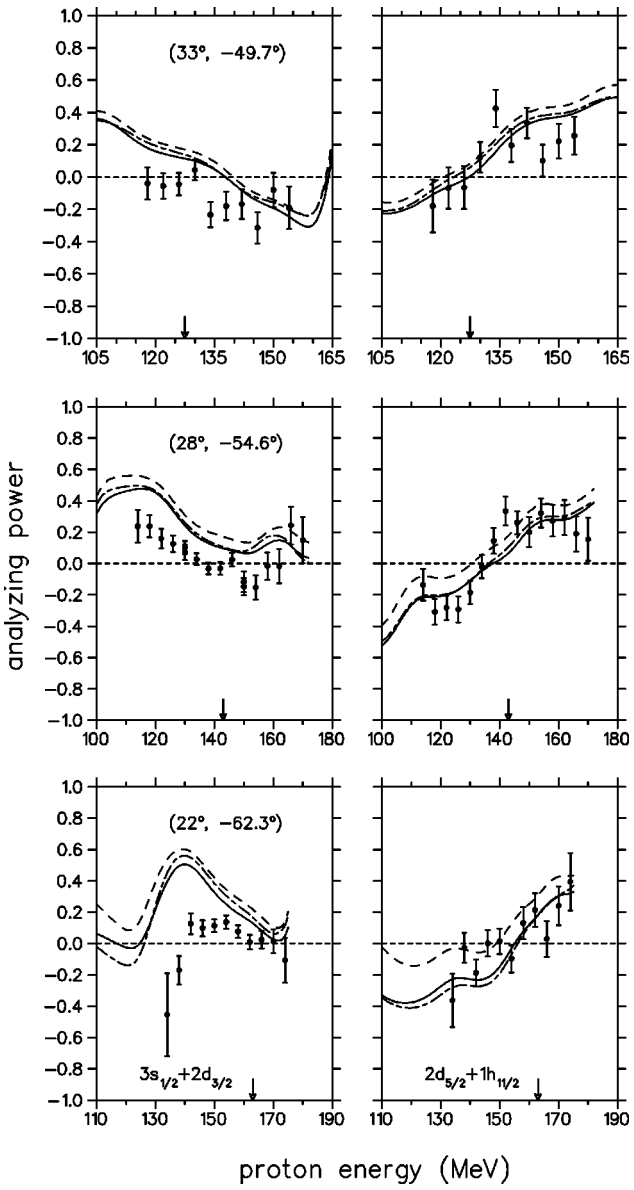

FIG. 7. Analyzing power energy-sharing distributions for the unresolved valence states. The curves represent DWIA predictions for the optical potential parameter set of Hama *et al.* [27], utilizing the free nucleon-nucleon interaction (dashed line) and the density dependent interactions of Kelly and Wallace [35] (solid line) and Horowitz and Iqbal [36] (dot-dashed line).

of Hama *et al.* [27], and the effects observed for the influence of density dependence is similar for the other sets that were investigated. It is observed that the two methods of introducing the density dependence of the nucleon-nucleon interaction yield very similar results. Calculated cross sections are insensitive to the density dependence of the nucleon-nucleon interaction, and spectroscopic factors therefore remain largely unaffected. However, theoretical analyzing power energy distributions that include the density dependence of the nucleon-nucleon interactions are noticeably lower than those that utilize the free nucleon-nucleon interaction. Yet, for the $3s_{1/2}$ state and the combination of states that involves the $3s_{1/2}$ state, the disagreement with experimental data remains significant, while the reduction results in acceptable agreement in the case of the $2d_{5/2}$ state. Results for the $2d_{3/2}$ state appear adequate for the angle pair (28°, −54.6°), but unsatisfactory for the angle pair (22°, −62.3°). An interesting observation is that the difference between the free and density-dependent calculations for the $3s_{1/2}$ state increases as the scattering angle θ_{K600} is decreased. This is, of course, as expected from the radial localization calculations.

B. Distortion effects

In order to explore the problem with the $3s_{1/2}$ state further, the influence of proton distortions is investigated. Proton distortions for a heavy target such as ^{208}Pb are quite severe; the result is that cross sections are typically diminished to less than 5% of the plane-wave impulse approximation (PWIA) value. The distortions also dramatically alter the analyzing power from the plane-wave results, which then corresponds to the free nucleon-nucleon scattering value in the absence of a distorting potential. In the latter case the total energy and relative scattering angle at which the nucleon-nucleon interaction occurs remains approximately constant over the energy-sharing range; therefore, the resulting distortion-free analyzing power does not vary appreciably as a function of energy of the outgoing proton. Both the spin-orbit term of the distorting optical potential as well as the effective polarization of the knocked-out target nucleon, generated through the absorptive (imaginary) terms of the distorting optical potentials, introduces a reaction dependence on the spin orientation of the incoming protons. Because of the energy dependence of the optical potentials, asymmetries in cross sections for differently polarized incoming protons occur that vary with outgoing proton energy, giving rise to the fluctuation of the analyzing power A_y around the plane-wave value.

It is therefore instructive to observe the effect of the exclusion of the spin-orbit interaction in the entrance and/or exit channels, shown in Fig. 9. In the total absence of spin-orbit distortion it is observed that the analyzing power for the $3s_{1/2}$ state approaches the plane-wave limit, and no longer varies appreciably as a function of energy of the outgoing proton. It can also be said that the contribution to the shape of the analyzing power for especially the *s*-state knockout originates predominantly from the spin-orbit interaction between the projectile and initial nucleus. This follows from the fact that the contribution of the (real) spin-orbit potential relative to the central potential is more prominent at higher energies. On the other hand, the qualitative features of the analyzing power of the *d* states remain independent of whether the spin-orbit interaction is included in the generation of the distorted waves or not. Similar trends have been illustrated for calculations of the ^{208}Pb$(p,2p)$ reaction at 150 MeV [24].

The shape of the analyzing power for the $3s_{1/2}$ state is thus due to the spin-orbit part of the optical potential, whereas for the other $l \neq 0$ states both the spin-orbit term and the effective polarization (Maris effect) contribute. For the $2d_{3/2}$ state it is found that the Maris effect dominates over

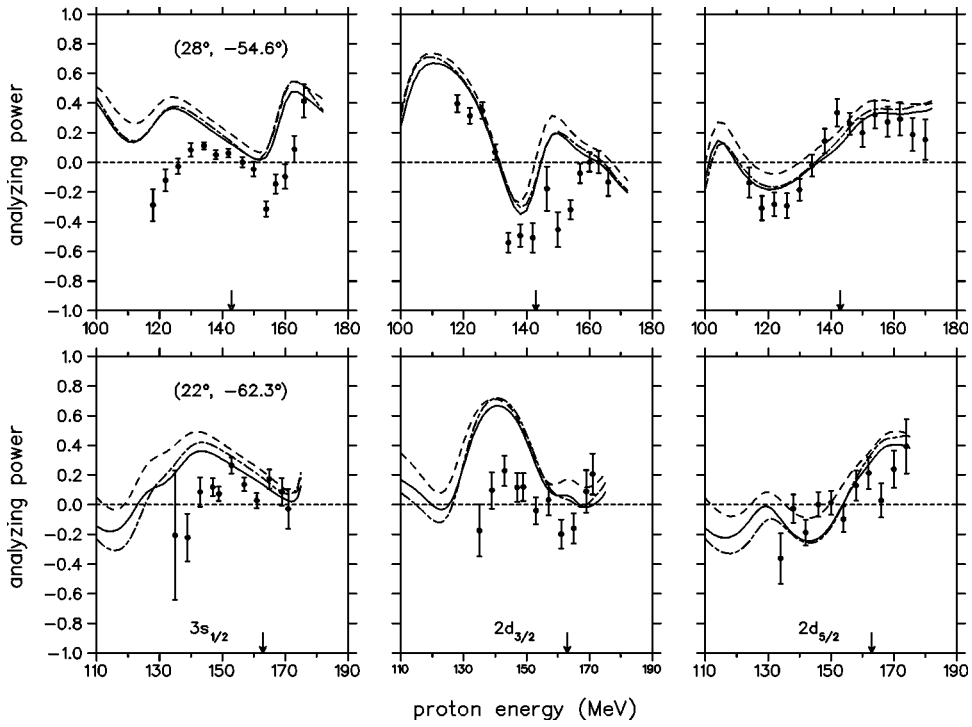

FIG. 8. Analyzing power energy-sharing distributions for the resolved valence states. The details of the calculations and notation of the curves are the same as in Fig. 7.

the contribution of the spin-orbit potential to A_y, whereas for the $2d_{5/2}$ state both sources of asymmetry contribute.

Because the spin-orbit potential plays such a prominent role in determining A_y of the *s* state, modifications to the spin-orbit interaction and its effect on the analyzing power requires further investigation, in order to rule out the possibility that this state of affairs is brought about by deficiencies common to all potential sets used. The physical significance of the real spin-orbit term is well established within the nonrelativistic framework. On the other hand, the imaginary spin-orbit term W_{so} has a dubious physical origin, and is said to merely represent a spin-dependent modification of the central imaginary potential, reducing absorption in the surface area [28,29]. Hence positive values for the imaginary term do not imply flux creation. This is in contrast with the Dirac equation based optical potential, where the imaginary spin-orbit potential appears as a natural consequence of the Dirac framework, and is shown to be critical to the fit of optical potential calculations to proton nucleus scattering data, even at low energies [49]. Thus, from the Hama potential we know that we need the imaginary spin-orbit term.

In Fig. 10 the effects on the analyzing power A_y for arbitrary changes to the imaginary spin-orbit potential is investigated, where $W'_{so}=a\times W_{so}$ with $a=(-1,0,1)$. Changing the sign of W_{so}, making it repulsive as in the case of the real spin-orbit term, clearly improves agreement of experiment with theoretical results. Although better agreement between theory and experimental data can be achieved by an arbitrary imaginary spin-orbit (W_{so}) term, the physical significance of this is clearly dubious, and it is therefore not pursued further. However, an interesting feature of the calculated analyzing powers of the *s* state for *all* the calculations featuring modified spin-orbit potentials is that variation in the spin-orbit potential has a negligible influence on the analyzing power at the point of minimum recoil. We conclude from this, similar to Miller *et al.* [17], that the consistent failure of the analyzing power prediction at the quasi-free point indicates that deficiencies of the optical potential alone cannot be blamed for the failure of the model.

C. Relativistic DWIA calculations

The initial failure of the DWIA to predict analyzing powers at 200 MeV [4,5] was solved by the relativistic finite-range DWIA calculations of Maxwell and Cooper [50,51] and Mano and Kudo [38]. This success at 200 MeV is in contrast with the failure of these calculations to achieve similar success at 500 MeV [13,17]. As a first test of the predictive powers of the relativistic distorted wave impulse approximation (RDWIA) for proton knockout from a heavy target at the projectile energy of 200 MeV, the relativistic finite-range DWIA calculation as modeled by Mano and Kudo [38] is compared with a nonrelativistic DWIA calculation.

Experimental results are compared with the RDWIA calculations performed with the code of Mano [37] in Fig. 11, compared to a representative density-dependent nonrelativistic DWIA calculation, using the second parametrization of the Dirac equation based potential as parametrized by Hama *et al.* [27], and the Kelly-Wallace nucleon-nucleon interaction [35].

For the cross-section distributions both the relativistic and nonrelativistic calculations yield similar agreement with the experimental values. The marked reduction observed compared to nonrelativistic DWIA calculations for the *s*-state analyzing power below 150 MeV for the angle pair (22°, −62.3°), and below 130 MeV for the angle pair (28°, −54.6°), is responsible for the improvement in agreement

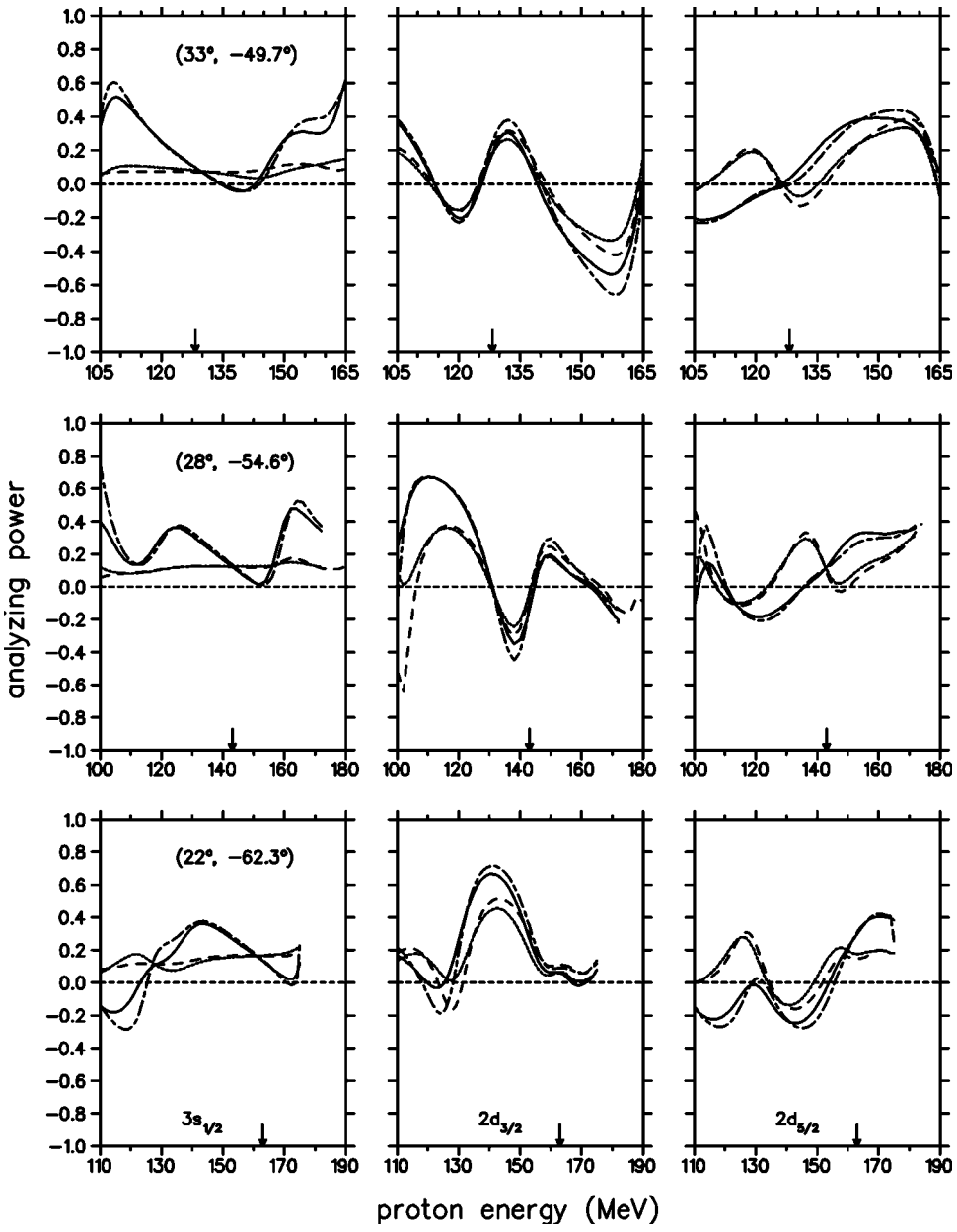

FIG. 9. Analyzing power energy-sharing distributions for the ground state and first two excited valence states for the optical model potential of Hama *et al.* [27] and the Kelly-Wallace [35] effective interaction (solid line), compared to calculations where the spin-orbit interaction is neglected for both incoming and outgoing channels (dashed line), for the incoming projectile only (small dashed line), and for the two outgoing protons only (dot-dashed line).

with all the experimental results. However, near the quasifree point it is found that the relativistic analyzing power calculations suffer from similar discrepancies with the experimental data as the nonrelativistic calculations. The results for the $2d_{3/2}$ state appear to be an ''attenuated'' version of the nonrelativistic analyzing power calculation, which leads to a better agreement for the $2d_{3/2}$ results for the angle pair (22°, $-62.3°$), while resulting in worse agreement with the experimental results from the angle pair ($28°, -54.6°$). The relativistic calculation also fails to give good predictions for the $2d_{5/2}$ state, perhaps even worse than the non-relativistic calculations.

Although the failure of RDWIA calculations in our case is not as spectacular as for the ^{16}O$(p,2p)$ reaction at 500 MeV [17], it is nevertheless a problem which was not observed for the quasifree scattering experiments at 200 MeV for the other targets (^{16}O,^{40}Ca). It should, however, be kept in mind that these calculations were done only for the free nucleon-nucleon interaction, and that density-dependent effects should be included before the RDWIA can be discarded as inappropriate.

V. SUMMARY AND CONCLUSION

High-resolution measurements for the ^{208}Pb$(\vec{p},2p)^{207}$Tl quasifree proton knockout reaction performed in this study show, as expected, that the standard nonrelativistic DWIA calculation yield a good shape agreement for the cross section results, as well as satisfactory spectroscopic factors. However, experimental analyzing power data for especially the $3s_{1/2}$ state exhibits a substantial reduction from the standard nonrelativistic DWIA calculations if the half-shell two-body scattering amplitude is approximated by the free nucleon-nucleon interaction. The inability of the DWIA to

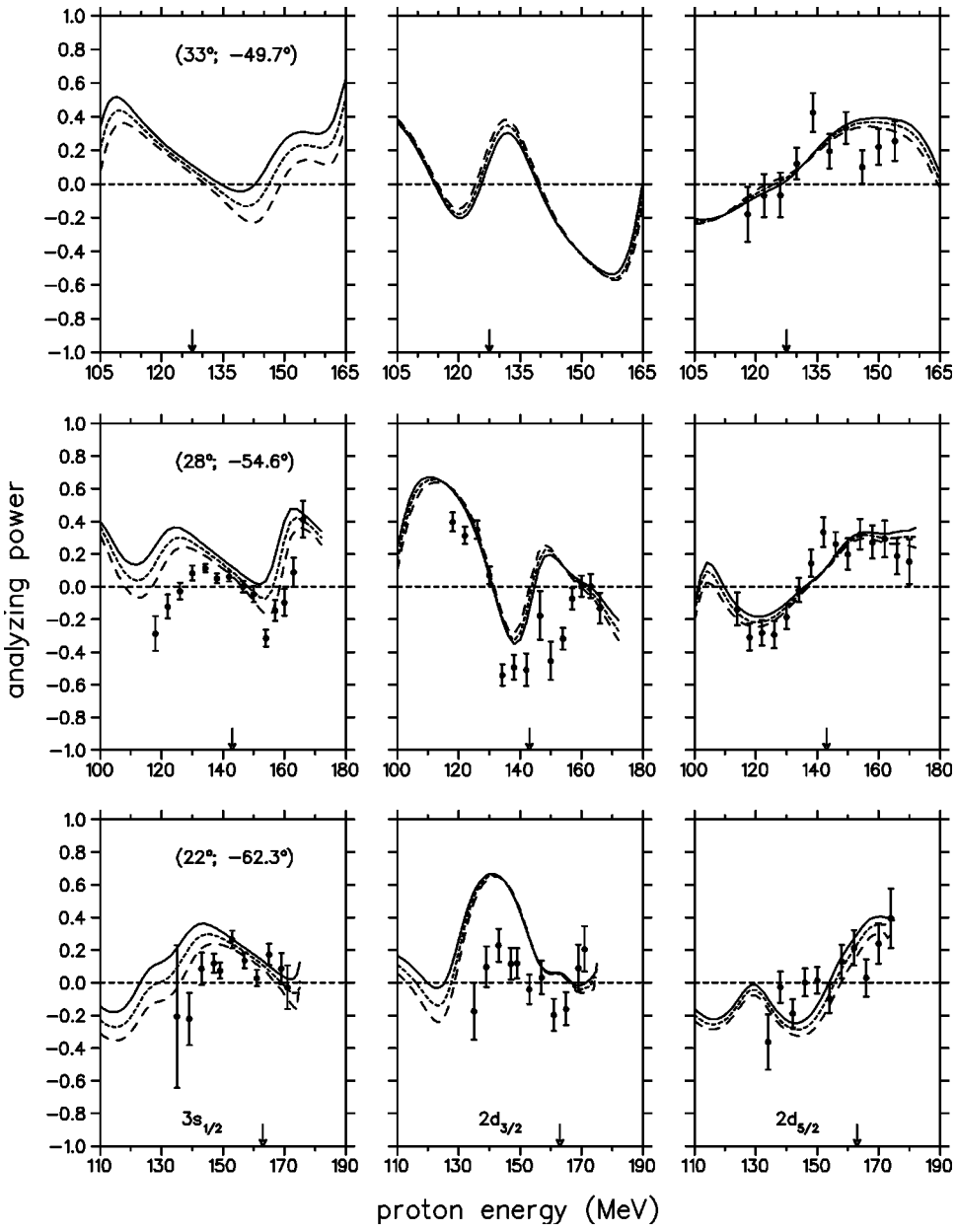

FIG. 10. Calculated analyzing power energy-sharing distributions for the $3s_{1/2}$, $2d_{3/2}$, and $2d_{5/2}$ states for the optical model potential of Hama *et al.* [27] and the Kelly-Wallace [35] effective interaction (solid line), compared to calculations with a modified version of the imaginary part of the spin-orbit potential: $W'_{so}=-W_{so}$ (dashed line) and $W'_{so}=0$ (dotted line).

predict analyzing powers accurately for light and medium targets is thus shown to persist in the high target-mass region.

One component of the DWIA calculation that is known to strongly affect the shape of the analyzing power is the optical potential used to generate the distortions of the proton wave functions. These distortions cause energy-dependent modifications to the corresponding PWIA analyzing power. For *s*-state knockout the modification of the corresponding PWIA analyzing power is due to the spin-orbit term of the optical potential, and more specifically due to the spin-orbit distortion of the projectile proton. It was shown that at the quasifree point, the analyzing power displays minimal sensitivity to changes in the spin-orbit potential term, which indicates that the observed analyzing power discrepancy is unlikely to be due to sensitivity to the distorting potentials. The deviation of the analyzing power for the *d* states from the PWIA value originates from both the spin-orbit potential terms as well as the effective initial spin polarization of the struck nucleon. No adjustment, within reason, to the different potential parameters of either the phenomenological Schrödinger or Dirac equation based optical potentials could resolve the discrepancy between experiment and theory. Because the distortions can only alter the shape of the PWIA analyzing power, without reducing the PWIA benchmark analyzing power, it is concluded that, in principle, the description of the proton distortions cannot account for the lowering of the analyzing power, needed to describe the data. Arguments that the reduction in A_y as observed at the higher energies is likely to be ascribed to inaccuracies in the parametrization of the standard phenomenological Schrödinger optical potentials (known to be less well determined at energies >200 MeV [52]) is thus shown to be unlikely.

It is clear that the mechanism required to improve agreement between experiment and theory must result in a reduced value for the calculated PWIA analyzing power over

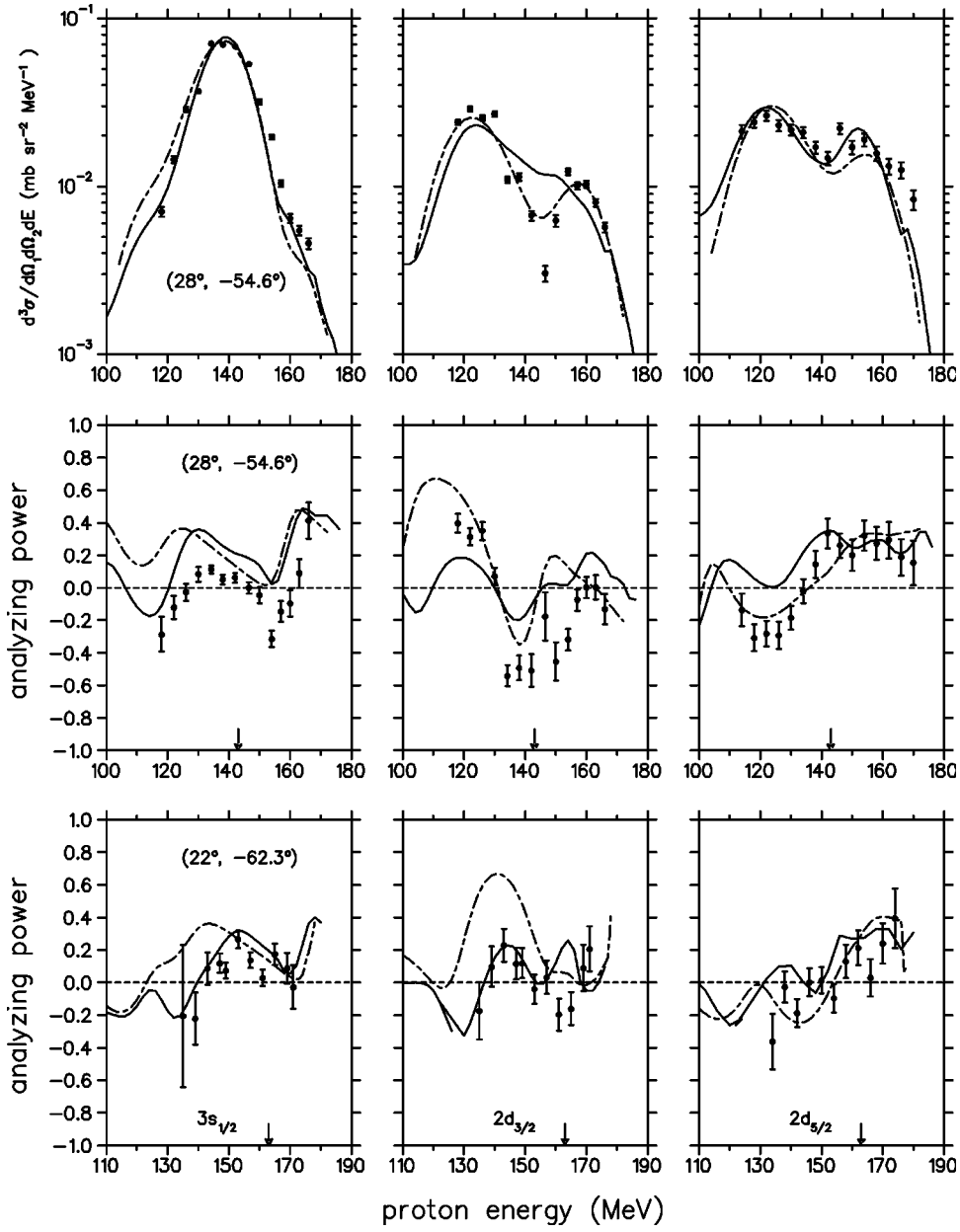

FIG. 11. Analyzing power and cross-section energy-sharing distributions for the resolved $3s_{1/2}$ and $2d_{3/2}$ states. Note that the results for the unresolved $(2d_{5/2}+1h_{11/2})$ states are compared to calculations for the $2d_{5/2}$ state only. Calculations shown are for the optical potential of Hama *et al.* [27] (DH2D) and the Kelly-Wallace [35] effective interaction (dot-dashed line), compared to calculations made with the RDWIA code of Mano (solid line).

the whole recoil momentum range. Other facets of the DWIA, such as the sensitivity to the energy prescription of the nucleon-nucleon interaction, as well as nonlocality effects, were investigated and shown to play a negligible role. Since the wave functions used for the bound protons are consistent with results from $(e,e'p)$ studies, it is concluded that the problem is unlikely to be caused by the description of the bound state wave function.

From the radial localization of the DWIA cross section it is seen that a small, though non-negligible contribution to the reaction originates from inside the nuclear volume. A medium modification to the nucleon-nucleon interaction is therefore a natural candidate in the search for mechanisms that cause changes in the analyzing power of the nucleon-nucleon interaction. The inclusion of density-dependent nucleon-nucleon interactions exhibited the desired trend in reducing the theoretical calculations over the whole range of recoil momenta. This reduction results in acceptable agreement between the theoretical prediction and experimental data for the $2d_{5/2}$ states, while the disagreement remains significant for the $3s_{1/2}$ state.

In order to ascertain whether a full relativistic calculation could provide a ready solution to the analyzing power problem, a standard relativistic DWIA (RDWIA) calculation was performed. Superficially the RDWIA calculation seems to provide much better results than the nonrelativistic calculations. However, whereas there is definitely improvement for the $3s_{1/2}$ state, agreement between the theoretical and experimental distributions for the other states deteriorates. Furthermore, the reduction near the quasifree point is as bad, or worse, as for the nonrelativistic calculations, indicating that the RDWIA is not more successful than the nonrelativistic DWIA. However, further calculations in which the density dependence is introduced are needed before a final conclu-

sion can be drawn concerning the success of the RDWIA.

To summarize: From the *cross-section* results of the $^{208}\mathrm{Pb}(\vec{p},2p)^{207}\mathrm{Tl}$ reaction at an incident energy of 202 MeV, we conclude that the DWIA is a reasonable theoretical framework for the description of quasifree proton scattering. However, discrepancies between experimental and theoretical *analyzing power* distributions indicate a need for refinements to the model. Furthermore, it is shown that a nuclear-matter density-dependent description of the nucleon-nucleon interaction inside the nuclear field is the only likely ingredient of the DWIA that allows an appropriate modification of the analyzing power. Available prescriptions for the introduction of a density dependence of the nucleon-nucleon interaction are reasonably successful, but the problem is not fully resolved, especially for knockout of protons from the *s*-state shell-model orbital. Clearly, further investigation of the theoretical formulation of this density dependence is needed.

ACKNOWLEDGMENTS

We thank G. J. Arendse, J. Bezuidenhout, J. J. Lawrie, R. Newman, W. A. Richter, F. D. Smit, and J. A. Stander for assistance during the collection of the experimental data. This work was performed with financial support from the South African National Research Foundation (NRF).

[1] P. Kitching, W.J. McDonald, A.J. Maris, and C.A.Z. Vasconcellos, Adv. Nucl. Phys. **15**, 43 (1985).
[2] S. Kullander, F. Lemeilleur, P.U. Renberg, G. Landaud, J. Yonnet, B. Fagerstrom, A. Johansson, and G. Tibell, Nucl. Phys. **A173**, 357 (1971).
[3] R.K. Bhowmik, C.C. Chang, P.G. Roos, and H.D. Holmgren, Nucl. Phys. **A226**, 365 (1974).
[4] P. Kitching, C.A. Miller, W.C. Olsen, D.A. Hutcheon, W.J. McDonald, and A.W. Stetz, Nucl. Phys. **A340**, 423 (1980).
[5] L. Antonuk, P. Kitching, C.A. Miller, D.A. Hutcheon, W.J. McDonald, G.C. Neilson, and W.C. Olsen, Nucl. Phys. **A370**, 389 (1981).
[6] W.T.H. van Oers, B.T. Murdoch, B.K.S. Koene, D.K. Hasell, R. Abegg, D.J. Margaziotis, M.P. Epstein, G.A. Moss, L.G. Greeniaus, J.M. Greben, J.M. Cameron, J.G. Rogers, and A.W. Stetz, Phys. Rev. C **25**, 390 (1982).
[7] C. Samanta, N.S. Chant, P.G. Roos, A. Nadasen, J. Wesick, and A.A. Cowley, Phys. Rev. C **34**, 1610 (1986).
[8] A.A. Cowley, J.J. Lawrie, G.C. Hillhouse, D.M. Whittal, S.V. Förtsch, J.V. Pilcher, F.D. Smit, and P.G. Roos, Phys. Rev. C **44**, 329 (1991).
[9] D.S. Carman, L.C. Bland, N.S. Chant, T. Gu, G.M. Huber, J. Huffman, A. Klyachko, B.C. Markham, P.G. Roos, P. Schwandt, and K. Solberg, Phys. Lett. B **452**, 8 (1999).
[10] A.A. Cowley, G.J. Arendse, J.A. Stander, and W.A. Richter, Phys. Lett. B **359**, 300 (1995).
[11] Y. Kudo and K. Miyazaki, Phys. Rev. C **34**, 1192 (1986); Y. Kudo, N. Kanayama, and T. Wakasugi, *ibid.* **38**, 1126 (1988); **39**, 1162 (1989).
[12] Y. Ikebata, Phys. Rev. C **52**, 890 (1995).
[13] O.V. Maxwell and E.D. Cooper, Nucl. Phys. **A603**, 441 (1996).
[14] P. Li, Ph.D. thesis, Indiana University, 1994.
[15] J.D. Huffman, Ph.D. thesis, University of Maryland, 1996.
[16] D.S. Carman, L.C. Bland, N.S. Chant, T. Gu, G.M. Huber, J. Huffman, A. Klyachko, B.C. Markham, P.G. Roos, P. Schwandt, and K. Solberg, Phys. Rev. C **59**, 1869 (1999).
[17] C.A. Miller, K.H. Hicks, R. Abegg, M. Ahmad, N.S. Chant, D. Frekers, P.W. Green, L.G. Greeniaus, D.A. Hutcheon, P. Kitching, D.J. Mack, W.J. McDonald, W.C. Olsen, R. Schubank, P.G. Roos, and Y. Ye, Phys. Rev. C **57**, 1756 (1998).
[18] K. Hatanaka, M. Kawabata, N. Matsuoka, Y. Mizuno, S. Morinobu, M. Nakamura, T. Noro, A. Okihana, K. Sagara, K. Takahisa, H. Takeda, K. Tamura, M. Tanaka, S. Toyama, H. Yamazaki, and Y. Yuasa, Phys. Rev. Lett. **78**, 1014 (1997); T. Noro, T. Baba, K. Hatanaka, M. Ito, M. Kawabata, N. Matsuoka, Y. Mizuno, S. Morinobu, M. Nakamura, A. Okihana, K. Sagara, H. Sakaguchi, K. Takahisa, H. Takeda, A. Tamii, K. Tamura, M. Tanaka, S. Toyama, H. Yamazaki, Y. Yuasa, Y. Yoshido, and M. Yosoi, Nucl. Phys. **A629**, 324c (1998).
[19] T. Noro, H. Akimune, H. Akiyoshi, I. Daito, H. Fujimura, K. Hatanaka, F. Ihara, T. Ishikawa, M. Itoh, M. Kawabata, T. Kawabata, Y. Maeda, N. Matsuoka, S. Morinobu, M. Nakamura, E. Obayashi, A. Okihana, K. Sagara, H. Sakaguchi, H. Takeda, T. Taki, A. Tamii, K. Tamura, H. Yamazaki, Y. Yoshido, M. Yoshimura, and M. Yosoi, in *Proceedings of the RCNP International Symposium on Nuclear Responses and Medium Effects*, Osaka, Japan, 1998, edited by T. Noro, H. Sakaguchi, H. Sakai, and T. Wakasa (Universal Academy, Tokyo, 1999), p. 167.
[20] G. Jacob, A.J. Maris, C. Schneider, and M.R. Teodoro, Phys. Lett. **45B**, 181 (1973).
[21] J.V. Pilcher, A.A. Cowley, D.M. Whittal, and J.J. Lawrie, Phys. Rev. C **40**, 1937 (1989).
[22] M.J. Martin, Nucl. Data Tables **70**, 315 (1993).
[23] N.S. Chant and P.G. Roos, Phys. Rev. C **15**, 57 (1977).
[24] N.S. Chant and P.G. Roos, Phys. Rev. C **27**, 1060 (1983).
[25] N. S. Chant and P. G. Roos, program THREEDEE, University of Maryland (unpublished).
[26] E.F. Redish, G.J. Stephenson, and G.M. Lerner, Phys. Rev. C **2**, 1665 (1970).
[27] S. Hama, B.C. Clark, E.D. Cooper, H.S. Sherif, and R.L. Mercer, Phys. Rev. C **41**, 2737 (1990).
[28] P. Schwandt, H.O. Meyer, W.W. Jacobs, A.D. Bacher, S.E. Vigdor, M.D. Kaitchuck, and T.R. Donoghue, Phys. Rev. C **26**, 55 (1982).
[29] A. Nadasen, P. Schwandt, P.P. Singh, W.W. Jacobs, A.D. Bacher, P.T. Debevec, M.D. Kaitchuck, and J.T. Meek, Phys. Rev. C **23**, 1023 (1981).
[30] F. Perey and B. Buck, Nucl. Phys. **32**, 353 (1962).
[31] C. Mahaux and R. Sartor, Nucl. Phys. **A481**, 381 (1988).
[32] E.N.M. Quint, Ph.D. thesis, University of Amsterdam, 1988 (unpublished).
[33] Z.Y. Ma and J. Wambach, Phys. Lett. B **256**, 1 (1991).
[34] R.A. Arndt and D. Roper, Virginia Polytechnic Institute and

State University Scattering Analysis Interactive Dial-In Program (SAID), Solution WI86.
[35] J.J. Kelly and S.J. Wallace, Phys. Rev. C **49**, 1315 (1994).
[36] C.J. Horowitz and M.J. Iqbal, Phys. Rev. C **33**, 2059 (1986).
[37] J. Mano, Program RELP2P, Osaka Prefectural College of Technology (unpublished).
[38] J. Mano and Y. Kudo, Prog. Theor. Phys. **100**, 91 (1998).
[39] C.J. Horowitz, Phys. Rev. C **31**, 1340 (1985).
[40] E.N.M. Quint, J.F.J. van den Brand, J.W.A. den Herder, E. Jans, P.H.M. Keizer, L. Lapikás, G. van der Steenhoven, P.K.A. de Witt Huberts, S. Klein, P. Grabmayr, G.J. Wagner, H. Nann, B. Frois, and D. Goutte, Phys. Rev. Lett. **57**, 186 (1986).
[41] D. Royer, M. Arditi, L. Bimbot, H. Doubre, N. Frascaria, J.P. Garron, and M. Riou, Nucl. Phys. **A158**, 516 (1970).
[42] J.P. McDermott, Phys. Rev. Lett. **65**, 1991 (1990).
[43] Y. Jin, D.S. Onley, and L.E. Wright, Phys. Rev. C **45**, 1311 (1992).
[44] J.M. Udìas, P. Sarriguren, E. Moya de Guerra, E. Garrido, and J.A. Caballero, Phys. Rev. C **48**, 2731 (1993).
[45] V.R. Pandharipande, C.N. Papanicolas, and J. Wambach, Phys. Rev. Lett. **53**, 1133 (1984).
[46] C. Mahaux and R. Sartor, Adv. Nucl. Phys. **20**, 1 (1991).
[47] N. Kanayama, Y. Kudo, H. Tsunoda, and T. Wakasugi, Prog. Theor. Phys. **83**, 540 (1990).
[48] C.W. Wang, N.S. Chant, P.G. Roos, A. Nadasen, and T.A. Carey, Phys. Rev. C **21**, 1705 (1980).
[49] E.D. Cooper, S. Hama, B.C. Clark, and R.L. Mercer, Phys. Rev. C **47**, 297 (1993).
[50] O.V. Maxwell and E.D. Cooper, Nucl. Phys. **A513**, 584 (1990).
[51] O.V. Maxwell and E.D. Cooper, Nucl. Phys. **A565**, 740 (1993).
[52] E. Bauge, J.P. Delaroche, and M. Girod, Phys. Rev. C **58**, 1118 (1998).